Novel *p*-Arylthio Cinnamides as Antagonists of Leukocyte Function-Associated Antigen-1/Intracellular Adhesion Molecule-1 Interaction. 2. Mechanism of Inhibition and Structure-Based Improvement of Pharmaceutical Properties

Gang Liu,*,† Jeffrey R. Huth,*,‡ Edward T. Olejniczak,‡ Renaldo Mendoza,‡ Peter DeVries,† Sandra Leitza,† Edward B. Reilly,† Gregory F. Okasinski,† Stephen W. Fesik,‡ and Thomas W. von Geldern†

Metabolic Disease Research and Research NMR, Pharmaceutical Products Division, Abbott Laboratories, Abbott Park, Illinois 60064-6098

Received November 27, 2000

The interaction between leukocyte function-associated antigen-1 (LFA-1) and intracellular adhesion molecule-1 (ICAM-1) has been implicated in inflammatory and immune diseases. Recently, a novel series of *p*-arylthio cinnamides has been described as potent antagonists of the LFA-1/ICAM-1 interaction. These compounds were found to bind to the I domain of LFA-1 using two-dimensional NMR spectroscopy of ^{15}N-labeled LFA-1 I domain. On the basis of NOE studies between compound **1** and the I domain of LFA-1, a model of the complex was constructed. This model revealed that compound **1** does not directly inhibit ICAM-1 binding by interacting with the metal ion dependent adhesion site (MIDAS). Instead, it binds to the previously proposed I domain allosteric site (IDAS) of LFA-1 and likely modulates the activation of LFA-1 through its interaction with this regulatory site. A fragment-based NMR screening strategy was applied to identify small, more water-soluble ligands that bind to a specific region of the IDAS. When incorporated into the parent cinnamide template, the resulting analogues exhibited increased aqueous solubility and improved pharmacokinetic profiles in rats, demonstrating the power of this NMR-based screening approach for rapidly modifying high-affinity ligands.

Introduction

Leukocyte function-associated antigen-1 (LFA-1) ($\alpha_L\beta_2$, CD11a/CD18) is a heterodimeric transmembrane glycoprotein expressed on all leukocytes.[1,2] As a cell-surface adhesion receptor, LFA-1 supports inflammatory and specific T-cell immune responses through mediating cell adhesion, leukocyte transmigration, and augmentation of T-cell receptor signaling.[3] These functions are achieved through an interaction with its counter-receptors—the intracellular adhesion molecules (ICAM)-1, -2, and -3 located on endothelial and antigen-presenting cells.[4,5] Therapeutic prevention of LFA-1 binding to ICAMs has potential in the treatment of inflammatory diseases[6] and graft rejection after transplantation.[7]

Similar to other integrins, LFA-1 consists of a large α-subunit (CD11a) and a smaller *β*-subunit (CD18). The most extracellular portion of the α-subunit of LFA-1 contains a magnesium cation-binding domain, called metal ion dependent adhesion site (MIDAS), which is involved in the direct interaction with ICAMs.[8] Near the amino terminus of the α-subunit is a 200 amino acid insert termed the I domain that is required for binding to ICAMs.[3] In the crystal structures of CD11b I domains, the I domain exhibited two different conformations depending on the crystal contacts.[8] This led to the proposal that one of the observed conformations is a mimetic of the "activated" ligand bound form while the other represents the unligated state of the protein. Differences in the conformation of CD11a I domain were also observed in crystallography studies.[9,10] The proposal that these conformations reflect a regulatory site was supported by a recent structural study of an I domain of $\alpha_2\beta_1$/collagen peptide complex in which the ligated I domain is in the proposed "activated" form.[11] In the "activated" ligand bound state, the C-terminal helix of the I domain drops downward by 10 Å, whereas in the unligated state, this helix moves away from the *β*-sheet core of the protein to expose a hydrophobic cleft. On the basis of a series of site-directed mutagenesis studies of amino acid residues in this cleft, we proposed that this site (termed the I domain allosteric site or IDAS) could act as a regulatory site for the activation process.[12]

Recently, a novel series of *p*-arylthio cinnamide-based antagonists of the LFA-1/ICAM-1 interaction has been reported by our laboratories, represented by **1** (Chart 1).[13] This series of compounds was identified by screening for the inhibition of the LFA-1/ICAM-1 interaction using full length proteins. In this report, we present the results of NMR studies that defined the binding site of these compounds. We also describe a rapid synthetic approach for investigating the A-ring SAR of the *p*-arylthio cinnamide antagonists and show how a fragment-based NMR screening approach facilitated the discovery of antagonists with improved pharmaceutical properties.

* Address correspondence to Gang Liu at D-47R, AP-10, Abbott Laboratories, 100 Abbott Park Road, Abbott Park, IL 60064-6098. Tel: (847) 935-1224, Fax: (847) 938-1674, E-mail: gang.liu@abbott.com. Address correspondence regarding NMR spectroscopy to Jeffrey R. Huth at D-47G, AP10, Abbott Laboratories, 100 Abbott Park Road, Abbott Park, IL 60064-6098. Tel: (847) 938−0959, Fax: (847) 938−2478, E-mail: jeff.huth@abbott.com.

† Metabolic Disease Research.

‡ Research NMR.

10.1021/jm000503f CCC: $20.00
Published on Web 03/21/2001

Chart 1. Representative Examples of the Diaryl Sulfides as LFA-1/ICAM-1 Antagonists

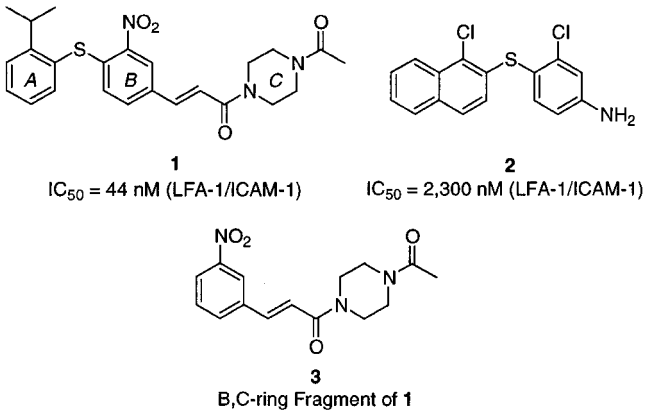

Chemistry

To expedite the exploration of different types of heterocycles for replacing the *i*-propylphenyl of **1**, a versatile synthetic sequence involving Ullmann coupling was devised (Scheme 1). Aromatic nucleophilic substitution of 3-chloro-4-fluorobenzaldehyde (**4**) with methyl 3-mercaptopropionate yielded the aldehyde **5**, which was converted to the cinnamide **6**. The masked benzenethiol was released by treatment of **6** with potassium *tert*-butoxide to give potassium thiolate **7** for the Ullmann coupling. Two types of coupling conditions have been tried with 5-iodoindole, both of which yielded sufficient amount of the desired product **8** for SAR studies, albeit in low yields.[14,15] The resulting indole analogue **8** could be further functionalized to give compounds **9** and **10** through Mannich reaction or simple alkylation, respectively.

The potassium thiolate **7** can also be used for nucleophilic substitution to give the nitro-containing compound **11** (Scheme 2). Reduction of the nitro group and cyclization of the resulting dianilino compound provided the benzimidazolone analogue **12**.

Results and Discussion

NMR Screening. Because of the central importance of the I domain for LFA-1 function, we reasoned that the small molecule antagonists identified by high-throughput screening may exert their functions by binding to the I domain. To test this hypothesis, two-dimensional ^{15}N-heteronuclear single-quantum correlation (^{15}N/^{1}H HSQC) spectra[16] of uniformly ^{15}N-labeled LFA-1 I domain[12] were recorded in the presence and absence of the original diaryl sulfide lead **2** (Chart 1).

Scheme 1[a]

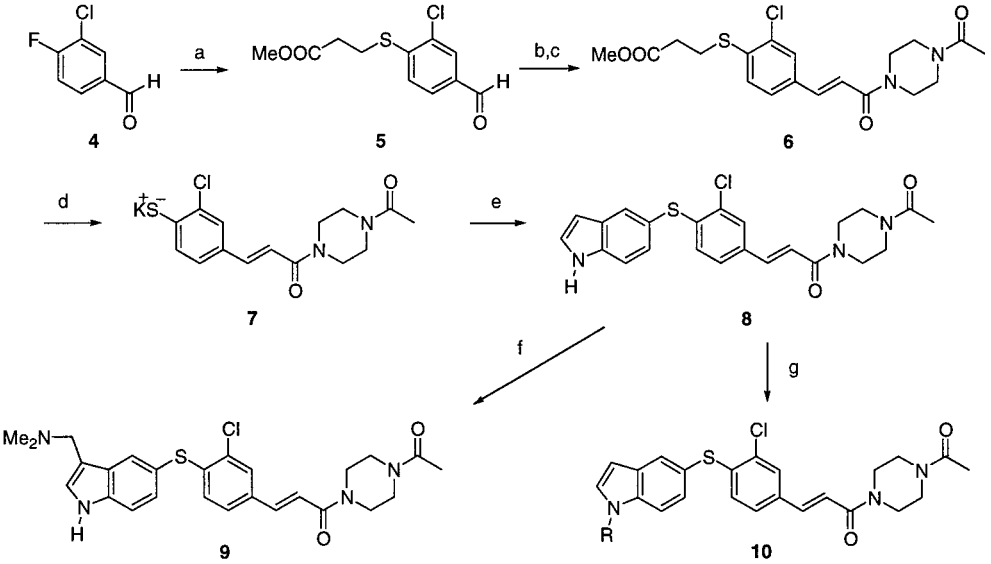

[a] Reagents and conditions: (a) K_2CO_3, $HSCH_2CH_2CO_2Me$, DMF, 70 °C, 95%; (b) malonic acid, cat. piperidine, pyr., 110 °C, 98%; (c) i. $(COCl)_2$, CH_2Cl_2, cat. DMF, rt; ii. *N*-acetylpiperazine, NEt_3, cat. DMAP, CH_2Cl_2, 84% two steps; (d) *t*-BuOK, THF, −78 °C−rt; (e) Cu powder, CuI, K_2CO_3, DMF, 90 °C, 25% or $Pd(PPh_3)_4$, *n*-BuOH, 100 °C, 22%; (f) $CH_2{=}N(CH_3)_2I$, dioxane/H_2O, rt, 59%; (g) KOH, DMSO, R−X, rt, 63%.

Scheme 2[a]

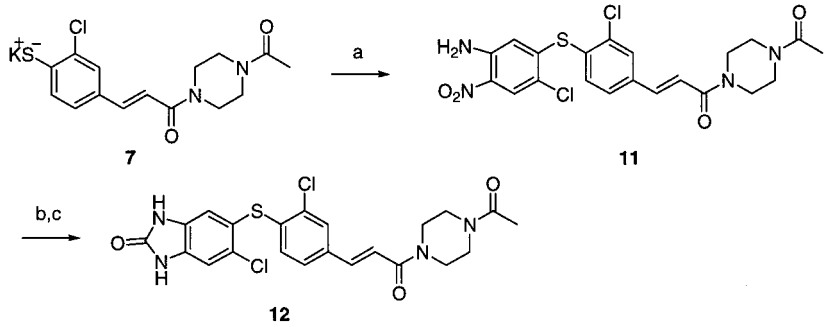

[a] Reagents and conditions: (a) 4,5-Dichloro-2-nitroaniline, K_2CO_3, DMF, 70 °C, 93%; (b) $SnCl_2$, EtOH, reflux, 44%; (c) CDI, reflux, THF, 32%.

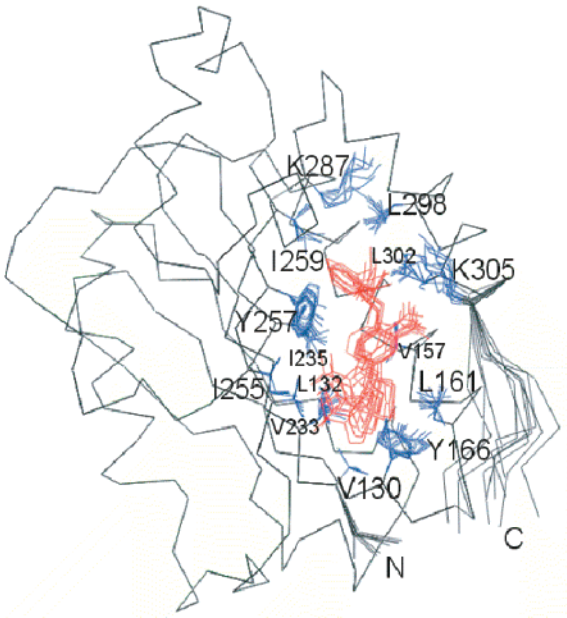

Figure 1. Backbone atom superposition of 10 models of compound **1** bound to the CD11a I domain. The protein backbone is shown in black, compound **1** in red, and protein side chains that create the binding pocket in blue.

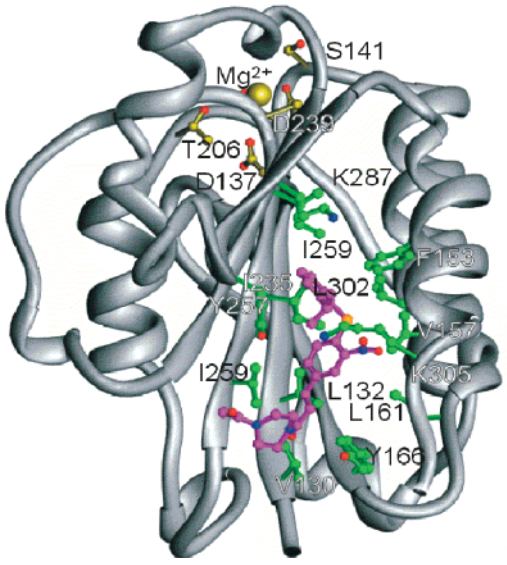

Figure 2. Average model of the CD11a I domain/compound **1** complex. Side chains of the IDAS that contact **1** are shown in green with nitrogens in blue and oxygens in red. Side chains of the MIDAS that chelate magnesium are shown in yellow with oxygens in red. Compound **1** is drawn in magenta with nitrogens in blue, oxygens in red, and the sulfur in gold. This figure was created using the program Ribbons (Carson, M. J. *J. Mol. Graph.* **1987**, *5*, 103−106).

Chart 2. Fragments Identified from NMR Screening in the Presence of Compound **3**

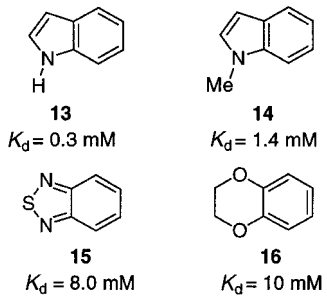

Numerous chemical shift changes were observed upon the addition of **2**, indicating that the diaryl sulfide binds to the I domain of LFA-1. NMR titration studies showed that compound **2** is in intermediate exchange which corresponds to a dissociation constant (K_d) less than 20 μM (K_d values for tight binders cannot be determined by NMR). This is consistent with the measured IC_{50} of 2.3 μM in the LFA-1/ICAM-1 binding assay using the entire extracellular domain of LFA-1. Compound **1** was found to be in slow exchange when titrated with the I domain, indicating a tighter binding than that of compound **2**, which was reflected as higher potency of compound **1**. That compound **1** also shifts similar resonances as compound **2** indicates both compounds bind to a similar region of the LFA-1 I domain. Thus, the interaction of the *p*-arylthio cinnamides with the I domain of LFA-1 can account for the inhibition of the full length LFA-1 protein without invoking binding to another site on LFA-1.

The location of the binding site within the I domain for this series of compounds was identified by NMR. Backbone and side chain assignments of the I domain and the I domain/**1** complex were obtained using standard heteronuclear multidimensional NMR experiments (Experimental Section). Nineteen NOEs between **1** and the I domain were obtained and assigned to residues within the IDAS of the I domain. Structure calculations using these NOEs and the X-ray coordinates for the free I domain[12] unambiguously determined the binding site and orientation of compound **1** within the IDAS (Figure 1). The model reveals that compound **1** binds to a hydrophobic pocket formed by strands one, three, and four of the core β-sheet and α-helices one and seven (Figure 2). Ring A of compound **1** interacts with a hydrophobic surface involving Ile259 and Ile235. The isopropyl substitution on ring A points away from the I domain pocket toward the hydrophobic portions of Lys287 and Lys305 on the surface of the I domain. The sulfur of compound **1** is buried within the hydrophobic pocket near Val157 and Leu302. Ring B is also buried in the hydrophobic pocket and shows NOE contacts to both residues Leu161 and Leu132. The ethenylcarbonyl group and attached *N*-acetylpiperazine point toward the N- and C-termini of the I domain, as indicated by the NOEs observed between the acetyl methyl group and Ile255. The absence of any NOEs to amino acid residues within the MIDAS proved that no direct interaction with the MIDAS by compound **1** was observed.

The binding of the *p*-arylthio cinnamide **1** to the IDAS of LFA-1 suggests an indirect mechanism of inhibition of the LFA-1/ICAM-1 interaction. Rather than directly inhibiting ICAM-1 binding by blocking the MIDAS of LFA-1, this series of compounds appears to act by disrupting a regulatory site that encompasses a deep hydrophobic pocket in the I domain of LFA-1. Lovastatin (**30**) (Chart 3) has recently been found to be an antagonist of the LFA-1/ICAM-1 interaction,[17] and its binding site has been determined using both NMR and X-ray crystallography. A superposition of our model with the X-ray structure of lovastatin complex shows that **30** and **1** bind in a similar manner (Figure 3). The RMSD of the protein backbones between the lovastatin complex and the complex **1** is 0.6 Å, and the position of the

Chart 3. Structure of Lovastatin, a Reported LFA-1/ICAM-1 Interaction Antagonist

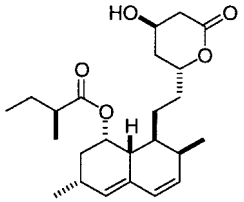

30

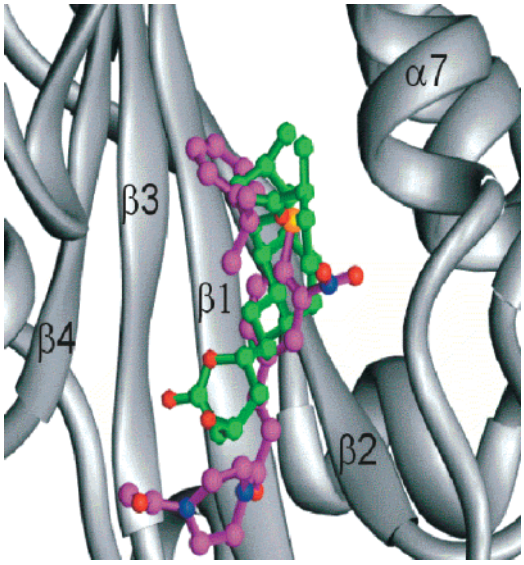

Figure 3. Superposition of compound **1** and lovastatin in the IDAS of LFA-1. Compound **1** is drawn in magenta with nitrogens in blue, oxygens in red, and the sulfur in gold. Lovastatin **30** (lactone form) is drawn in green with oxygens in red.

C-terminal helix is in the conformation of the "unligated" I domain for both complexes. Secondly, rings B and C of **1** occupy the same space in the IDAS as does **30**. These results show that blocking LFA-1 activation through this IDAS site can be achieved with different molecular scaffolds by locking the I domain in a low-avidity conformation.

Fragment-Based NMR Screening To Optimize Compound 1. It has recently been shown that high-affinity ligands can be designed by using information derived from the NMR-based screening of fragments.[18] The method involves the fragmentation of an existing lead molecule, the identification of suitable replacements for the fragments, and incorporation of the newly identified fragments into the original scaffold. In the case of the *p*-arylthio cinnamide, the presence of hydrophilic residues L287 and L305 in the A-ring binding pocket offered opportunities to improve the potency and physical properties of **1** through identification of more hydrophilic replacements of the *i*-propylphenyl moiety.

Toward this end, compound **3** (Chart 1) was synthesized as a fragment of **1** to block the binding sites for the B- and C-rings on the I domain. Subsequently, 2500 molecules with a molecular weight less than 150 Da were tested for binding to the I domain in the presence of saturating amounts of **3**. Several classes of heterocycles were identified which bind to the A-ring site with K_d values in the submillimolar to millimolar range, including indole (**13**), *N*-methylindole (**14**), 2,1,3-benzothiadiazole (**15**), and benzodioxane (**16**) as shown in Chart 2. NMR structural studies indicate that these molecules bind to the A-ring site. For instance, NMR experiments on a ternary complex of compound **3** and **16** bound to the I domain revealed NOEs between compound **16** and residue Ile259 of the IDAS. This indicates that compound **16** binds to the pocket occupied by the A-ring of the parent compound **1**. NOEs between compound **3** and methyl groups of the IDAS were also observed, indicating that **3** and **16** bind to the IDAS in the same region as the parent compound **1**.

With A-ring replacement fragments identified, a strategy was needed for the final assembly of the linked molecules. From the previous A-ring SAR study for increasing aqueous solubility with heterocycles, it was determined that when the sulfide is linked to the heteroatom-containing rings, the resulting compounds exhibited dramatically decreased potency.[19] This information led to the strategy of linking to the benzo portion of the A-ring replacement fragments. Indole fragment **13** was used to explore the effect of different positions for the sulfide bond. Linking at the 5-position of the indole yielded compound **8** which possessed slightly improved potency compared to **1** (Table 1). The hydrogen-bonding character of the indole does not appear to be important because the *N*-methylated indole yielded an equipotent compound **10a**. Linking at the 6-position of the indole resulted in compound **17** which displayed greater than 7-fold decrease in potency versus the 5-position analogue **8**. *N*-Methylindole linked at the 7-position (**18**) is over 3-fold less potent than the 5-*N*-methylated analogue **10a**, while ethylation further decreased the potency of the resulting compound **19**. So, the 5-position of indole appears to be the preferred position for forming the sulfide bond. Accordingly, methylenedioxybenzene, a bioisoster of benzothiadiazole,[20] was linked at the 5-position to provide **20** which possessed a 3-fold loss of potency compared with **1**. In addition, the benzodioxane was linked at the 6-position to yield **21** (A-292949) with comparable potency as **1**. The NOE evidence suggests that the aromatic portion of the benzodioxane packs against the side chain of I259. This orientation would allow the dioxane to point toward the solvent where the interactions with water and the side chains of L287 and L305 are possible.

It is interesting to note that, as fragments, indole and benzodioxane showed a 30-fold difference in binding affinity as estimated from NMR titration in the presence of **3**, yet the potencies of the corresponding linked compounds **8** and **21** differ by only 2-fold. It is not unexpected that variation exists before and after fragments being linked to the core structure. Introduction of a linker atom between two ligands may alter the binding orientation of the A- and B-rings relative to the unlinked fragments. Such a small change in binding orientation could account for the narrowing of 30-fold affinity difference to near equipotency for **8** and **21**.[21]

A cell-based adhesion assay, which measures the ability of the antagonists to block the adherence of JY-8 cells expressing LFA-1 to immobilized ICAM-1, was used to confirm the functional activity in vitro. Among the more potent compounds listed in Table 1, indole compounds **8** and **10a** gave IC_{50} values of 15 nM and

Table 1. LFA-1/ICAM-1 Binding Inhibition from A-Ring Modification of the *p*-Arylthio Cinnamides

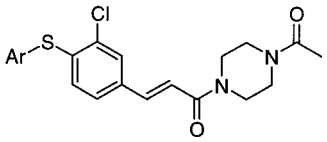

Compound	Ar	IC_{50} (nM)[a] (range)
8	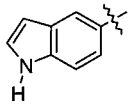	20 (20-30)
10a	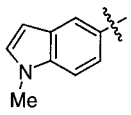	20 (20-30)
17	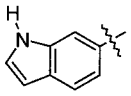	150 (100-230)
18	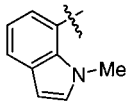	70 (70-80)
19	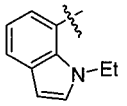	130 (120-140)
20	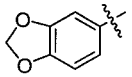	120 (110-140)
21	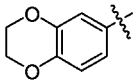	40 (30-60)

[a] IC_{50} calculated using a mean of at least two measurements (all duplicates) for six concentrations from 6.4×10^{-9} to 2×10^{-5} unless otherwise noted.

30 nM, respectively, while the benzodioxane analogue **21** exhibited an IC_{50} of 80 nM in this assay.

Attention was then turned to attaching more hydrophilic groups to the indole and benzodioxane portions of the molecules (Table 2). The *N*,*N*-dimethylaminomethyl-substituted indole analogue **9** exhibited over a 20-fold loss in potency compared to **8**. This loss in potency was partially recovered with *N*,*N*-dimethylaminomethyl-substituted indole analogue **22**. Attachment of a negatively charged carboxy group (**23**) to the methyl group of **10a** resulted in an over 15-fold loss of potency. Furthermore, the addition of a neutral methoxymethyl group (**24**) to the methyl group of **10a** led to 3-fold loss of potency.

For the benzodioxane-based analogue, addition of an ethoxy group to the 5-position of the benzodioxane of **21** resulted in **25** with over 2-fold decrease of potency (Table 2). Attaching a hydroxymethyl group to the 2/3-position of the benzodioxane yielded compound **26** which

Table 2. LFA-1/ICAM-1 Binding Inhibition from A-Ring Modification (Substituted Indoles and Benzodioxanes) of the *p*-Arylthio Cinnamides

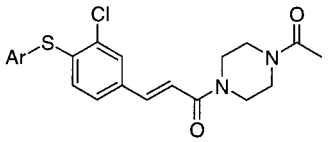

Compound	Ar	IC_{50} (nM)[a] (range)
9	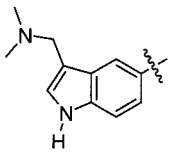	420 (370-470)
22	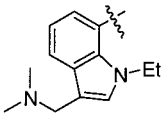	100 (100-110)
23	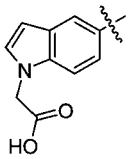	330 (320-350)
24	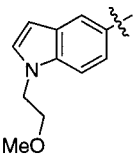	60 (30-60)
25	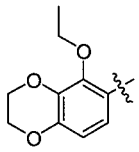	100 (90-110)
26[b]	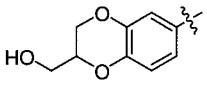	20 (20-30)
27[b]	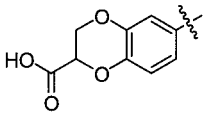	1,200 (1,000-1,500)
28[b]	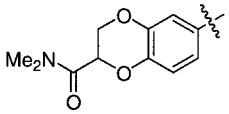	510
12	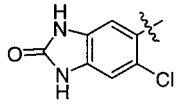	790 (728-860)
29	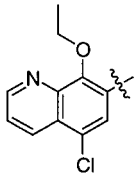	580

[a] IC_{50} calculated using a mean of at least two measurements (all duplicates) for six concentrations from 6.4×10^{-9} to 2×10^{-5} unless otherwise noted. [b] 1:1 mixture of 2- and 3-position regioisomers.

Table 3. Pharmacokinetic Profiles of Representative Compounds in Rats[a,b]

compd	solubility (μg/mL)	V_β (l/kg)	i.v. $t_{1/2}$ (h)	$AUC_{i.v.}$ (μg·h/mL)	oral C_{max}/T_{max} (μg/mL; h)	oral $t_{1/2}$ (h)	AUC_{oral} (μg·h/mL)	F (%)
1	0.9 ± 0.1	2.0 (1.1−3.0)	0.4 (0.3−0.9)	1.9 (1.8−2.1)	0	ND[c]	0	0
8	0.8 ± 0.1	i.v. dosing not possible			0.6/6.0 (0.4−0.8)/(4.0−8.0)	4.7 (4.1−5.5)	5.8 (4.2−8.8)	NA[c]
21	4.1 ± 0.5	3.0 (0.9−6.0)	0.55 (0.30−1.79)	2.2 (2.1−2.3)	0.19/0.5 (0.17−0.20)/(0.25−1.0)	1.1 (0.99−1.14)	0.28 (0.19−0.35)	12.4 (8.7−15.8)

[a] A total of 5 mg/kg dosed for both intravenous injection and oral gavage. [b] Harmonic mean from three rats each listed with the range of the data in parentheses. [c] ND, not determined. NA, not applicable.

exhibits a potency improvement over the parent compound **21**. In contrast, attachment of a carboxy group to the benzodioxane of **21** led to a 30-fold decrease of potency with the resulting analogue **27**. *N*,*N*-Dimethylcarboxamide attachment at the 2/3-position of the benzodioxane gave compound **28** which had a much reduced potency compared with compound **21**. Benzimidazolone-based compound **12** exhibited submicromolar potency, as did the quinoline-derived compound **29**.

The solubility and pharmacokinetic profiles of representative compounds were measured, and the results are shown in Table 3. The indole replacement of *i*-propylphenyl (**8**) did not improve the aqueous solubility over that of **1**, while the benzodioxane replacement (**21**) yielded at least 4-fold increase of aqueous solubility. Although the solubility improvement observed with the incorporation of heteroatoms did not appear to be dramatic, this modification did render an improvement in the rat pharmacokinetic profile of the resulting analogues over **1**. Compound **1** could not be detected following 5 mg/kg oral dosing in rats. In contrast, compound **8** (unable to dose i.v. due to poor solubility) was detected after oral dosing and yielded an oral half-life of 4.7 h. The oral AUC is 5.8 μg·h/mL after 5 mg/kg oral gavage in rats. The solubility improvement obtained for **21** enabled i.v. administration and yielded an oral bioavailability of ∼13%.

Conclusions

Using NMR, the binding site of compound **1** was established as the proposed IDAS of the I domain of LFA-1. The NMR studies suggest a possible mechanism of inhibition of the LFA-1/ICAM-1 interaction by our novel series of *p*-arylthio cinnamides that involves the disruption of a hydrophobic regulatory site of the I domain of LFA-1. The application of fragment-based NMR screening in combination with an Ullmann reaction-based divergent synthetic sequence significantly decreased the time and effort involved in modifying this series of high-affinity ligands. A-ring modification of compound **1** resulted in high-affinity antagonists of the LFA-1/ICAM-1 interaction, such as **21**, with increased aqueous solubility and improved pharmacokinetic profiles in rats. In addition, heterocycle-based A-ring replacements provided a diverse set of fragments that can be combined with the optimized B- and C-rings of the *p*-arylthio cinnamides, which will be reported in the following papers.

Experimental Section

General. Unless otherwise specified, all solvents and reagents were obtained from commercial suppliers and used without further purification. All reactions were performed under nitrogen atmosphere unless specifically noted. Flash chromatography was performed using silica gel (230−400 mesh) from E. M. Science. Proton NMR spectra were recorded on a General Electric QE300 instrument with Me_4Si as an internal standard and are reported as shift (multiplicity, coupling constants, proton counts). Mass spectral analyses were accomplished using desorption chemical ionization (DCI), atmospheric pressure chemical ionization (APCI), and electrospray ionization (ESI), as specified for individual compounds. Elemental analyses were performed by Robertson Microlit Laboratories, Madison, NJ, and are consistent with theoretical values to within 0.4% unless otherwise indicated. Preparative HPLC was performed on an automated Gilson HPLC system, using an YMC C-18 column, 75 × 30 mm i.d., S-5 μM, 120 Å, and a flow rate of 25 mL/min; λ = 214, 245 nm; mobile phase A, 0.05 M NH_4OAc or 0.1% TFA in H_2O, and mobile phase B, CH_3CN; linear gradient 20−100% of B in 20 min. The purified fractions were evaporated to dryness on a Savant SpeedVac.

Detection of Ligand Binding Using NMR. The I domain of LFA-1 was isotopically labeled and purified as previously described.[12] NMR samples contained 0.4 μM uniformly ^{15}N-labeled LFA-1 I domain, 0.6 mM $MgCl_2$, 100 mM sodium phosphate (pH 7.2) in H_2O/D_2O (9:1). Ligand binding was detected at 30 °C by acquiring sensitivity-enhanced [^{15}N]HSQC spectra[16] on a Bruker DRX500 spectrometer in the presence and absence of added compound. Dissociation constants were estimated by monitoring chemical shift changes as a function of added ligand.[22]

NOE-Based Model of LFA-1 I Domain/Compound 1 Complex. NMR experiments were performed at 30 °C on Bruker DRX spectrometers at 500, 600, and 800 MHz. Backbone and side chain assignments of the I domain in the absence of ligand were obtained as previously reported.[12] Assignments for the complex with compound **1** were obtained using similar experiments. Amides not able to be assigned with backbone triple resonance experiments were assigned using ^{15}N-edited NOE experiments. Carbon and proton assignments for methyl group were obtained from ^{13}C-edited NOE experiments using ^{15}N, ^{13}C, ^{2}H-labeled protein with protons incorporated at the γ-methyls of Val, δ-methyls of Leu, and β-, γ1-, γ2-, and δ1-positions of Ile.[23] NOEs between the ligand and protein were obtained from isotope-edited/filtered 3D experiments.[24] Ligand assignments were obtained from two-dimensional double-filtered NOESY and TOCSY experiments.[25]

A model of the complex was obtained by manually positioning compound **1** near the C-terminus of the I domain followed by energy minimization with the XPLOR.[26] In the calculations, the backbone atoms for residues 130−303 were fixed. The side chain atoms were allowed to move to accommodate the ligand. A total of 19 intermolecular and two intraligand distance restraints were used with a square well potential and placed into two loose distance categories, 1.8−5.0 and 1.8−6.0 Å. An additional angstrom was added to the upper limit for NOEs involving methyl groups of valine or leucine that were not stereoassigned. Two constraints were included to reflect the lack of an observed NOE. These constrains kept the closest approach for these pairs of protons at 4 Å.

Fragment-Based NMR Screening. ^{15}N-LFA-1 I domain (0.3 mM) in 0.45 mM $MgCl_2$ and 100 mM sodium phosphate (pH 7.0) in H_2O/D_2O (9:1), in the presence of 0.3 mM compound **3**, was analyzed with and without mixtures of five compounds

at 5 mM each. Compounds were added from 1 M stocks in deuterated DMSO. Ligand binding was detected by acquiring [^{15}N]HSQC spectra. To deconvolute mixtures that induced chemical shift changes of the I domain, binding of each of the five compounds was evaluated individually. Binding affinities for compounds that bind in the presence of compound **3** were determined by NMR as described previously.[22] Confirmation that these molecules bind to the pocket occupied by the A-ring of compound **1** was based on observed NOEs between compound **16** and the protein for a ternary complex composed of the I domain, compound **3**, and compound **16**.

3-[4-[3-(4-Acetyl-piperazin-1-yl)-3-oxo-propenyl]-2-chlorophenylsulfanyl]-propionic Acid Methyl Ester (6). To a stirred solution of 3-chloro-4-fluorobenzaldehyde (3.3 g, 20.8 mmol) in 25 mL of anhydrous DMF with potassium carbonate (4.3 g, 31.1 mmol) was added methyl-3-mercaptopropionate (2.3 mL, 20.8 mmol) via syringe dropwise. The mixture was then heated at 60 °C for 2 h. The reaction mixture was then cooled to room temperature and partitioned between ether and water. The aqueous layer was extracted with ether once, and the combined organic layer was washed with water and brine, dried over Na_2SO_4, and condensed in vacuo to give 5.1 g (19.7 mmol, 95%) of the desired aldehyde **5** as a colorless oil.

A mixture of the aldehyde **5** (1.0 g, 3.9 mmol), malonic acid (0.88 g, 8.5 mmol), and piperidine (57 μL, 0.58 mmol) in 4 mL of anhydrous pyridine was heated at 110 °C for 2 h during which the gas evolution ceased. After pyridine was removed under vacuum, water and 3 N aqueous HCl were then added with stirring. The desired cinnamic acid was collected through filtration, washed with cold water, and dried in a vacuum oven overnight to give 1.15 g (4.8 mmol, 98%) of the cinnamic acid as a white solid.

A suspension of the acid (220 mg, 0.73 mmol) in 5 mL of CH_2Cl_2 was stirred with $(COCl)_2$ (71 μL, 0.81 mmol) and one drop of DMF for 90 min. The solvent was then removed under vacuum, and the residual $(COCl)_2$ was removed with benzene (2 × 2 mL) in vacuo. A separate flask was charged with *N*-acetylpiperazine (113 mg, 0.88 mmol), NEt_3 (257 μL, 1.83 mmol), and DMAP (4.4 mg, 0.032 mmol) in 10 mL of CH_2Cl_2. The acid chloride in 5 mL of CH_2Cl_2 was then dropped in slowly. After 30 min, the reaction mixture was poured into 3 N aqueous HCl and extracted with EtOAc. The organic layer was washed with brine, dried with Na_2SO_4, and condensed under reduced pressure. The crude product was purified on a silica gel flash column (5−10% MeOH in EtOAc as eluent) to give 250 mg (0.61 mmol, 84%) of cinnamide **6** as a white solid. ^{1}H NMR ($CDCl_3$, 300 MHz) δ 2.16 (s, 3H), 2.72 (t, J = 7.5 Hz, 2H), 3.25 (t, J = 7.5 Hz, 2H), 3.54 (t, J = 4.95 Hz, 2H), 3.60−3.83 (brm, 6H), 6.83 (d, J = 15.6 Hz, 1H), 7.28 (d, J = 8.7 Hz, 1H), 7.37 (dd, J = 2.1, 8.7 Hz, 1H), 7.56 (d, J = 2.1 Hz, 1H), 7.61 (d, J = 15.6 Hz, 1H); MS (APCI$^+$) $(M + NH_4)^+$ at *m*/*z* 428, 430.

Potassium-4-[3-(4-acetyl-piperazin-1-yl)-3-oxo-propenyl]-2-chloro-benzenethiolate (7). To a stirred solution of the compound **6** (105 mg, 0.26 mmol) in 2 mL of THF at 0 °C was added *t*-BuOK solution (1.0 M, 281 μL, 0.29 mmol). Light orange precipitates appeared immediately. After completion of the addition, the reaction mixture was stirred at room temperature for 1 h before the solvent was removed on a rotavap under reduced pressure. The residue was dried under high vacuum to give the potassium thiolate **7** as a light yellow solid. ^{1}H NMR (DMSO-d_6, 300 MHz) δ 2.02 (s, 3H), 3.46 (brs, 6H), 3.54−3.80 (m, 2H), 6.88 (d, J = 14.9 Hz, 1H), 6.96 (d, J = 8.7 Hz, 1H), 7.26 (dd, J = 2.1, 8.7 Hz, 1H), 7.33 (d, J = 2.1 Hz, 1H), 7.46 (d, J = 14.9 Hz, 1H); MS (ESI$^+$) $(M + H)^+$ at *m*/*z* 324, 326.

5-Indolyl 2-Chloro-4-(*E*-((4-acetylpiperazin-1-yl)carbonyl)ethenyl)phenyl Sulfide (8). Method A of Sulfide Formation. To a stirred solution of 5-iodoindole (255 mg, 1.05 mmol) in 5 mL of anhydrous DMF were added the potassium thiolate **7** (457 mg, 1.26 mmol), followed by K_2CO_3 (174 mg, 1.26 mmol) and cuprous iodide (20 mg, 0.11 mmol). The resulting mixture was then heated at 120 °C overnight. The reaction mixture was then allowed to cool to ambient temperature and poured into water. The aqueous mixture was extracted with EtOAc (2 × 25 mL). The combined organic layer was then washed with water and brine, dried over Na_2SO_4, filtered, and concentrated. The crude product was purified using a Gilson preparative HPLC to give compound **8** (115 mg, 0.58 mmol, 25%) as an amorphous off-white solid. ^{1}H NMR (DMSO-d_6, 300 MHz) δ 2.03 (s, 3H), 3.40−3.78 (m, 8H), 6.51 (d, J = 8.4 Hz, 1H), 6.53 (s, 1H), 7.23 (dd, J = 2.1, 8.4 Hz, 1H), 7.27 (d, J = 15.6 Hz, 1H), 7.39 (d, J = 15.6 Hz, 1H), 7.41 (dd, J = 1.8, 8.4 Hz, 1H), 7.49 (t, J = 2.7 Hz, 1H), 7.56 (d, J = 8.4 Hz, 1H), 7.85 (d, J = 1.8 Hz, 1H), 7.99 (d, J = 1.8 Hz, 1H); MS (APCI$^+$) $(M + NH_4)^+$ at *m*/*z* 440, 442. Anal. ($C_{23}H_{22}ClN_3O_2S\cdot0.53CH_2Cl_2$) C, H, N.

3-(Dimethylaminomethyl)indol-5-yl 2-Chloro-4-(*E*-((4-acetylpiperazin-1-yl)carbonyl)ethenyl)phenyl Sulfide (9). To a stirred solution of Eschenmoser's salt (15 mg, 0.081 mmol) in 1 mL of dioxan/H_2O (3:1) at ambient temperature was added compound **8** (30 mg, 0.068 mmol). The mixture was then stirred at room temperature overnight. Solvent was then removed on a rotavap under reduced pressure, and the resulting crude product was purified on a Gilson preparative HPLC to give compound **9** as a light brown solid (20 mg, 0.040 mmol, 59%). ^{1}H NMR ($CDCl_3$, 300 MHz) δ 2.15 (s, 3H), 2.54 (s, 6H), 3.47−3.85 (m, 8H), 4.05 (s, 2H), 6.56 (d, J = 8.7 Hz, 1H), 6.77 (d, J = 15.6 Hz, 1H), 7.09 (d, J = 8.7 Hz, 1H), 7.36 (dd, J = 1.5, 8.7 Hz, 1H), 7.50 (d, J = 8.7 Hz, 1H), 7.52 (s, 2H), 7.56 (d, J = 15.6 Hz, 1H), 7.88 (s, 1H), 9.27 (s, 1H); MS (ESI$^+$) $(M + H)^+$ at *m*/*z* 497, 499. Anal. ($C_{26}H_{29}ClN_4O_2S\cdot1.24TFA$) C, H, N.

1-Methylindol-5-yl 2-Chloro-4-(*E*-((4-acetylpiperazin-1-yl)carbonyl)ethenyl)phenyl Sulfide (10a): white solid; ^{1}H NMR (DMSO-d_6, 300 MHz) δ 2.04 (s, 3H), 3.40−3.80 (m, 8H), 3.86 (s, 3H), 6.49 (d, J = 8.4 Hz, 1H), 6.52 (d, J = 3.0 Hz, 1H), 7.27 (d, J = 15.6 Hz, 1H), 7.31 (dd, J = 2.4, 8.4 Hz, 1H), 7.39 (d, J = 15.6 Hz, 1H), 7.41 (dd, J = 1.8, 8.4 Hz, 1H), 7.48 (d, J = 3.0 Hz, 1H), 7.63 (d, J = 8.4 Hz, 1H), 7.85 (d, J = 1.8 Hz, 1H), 7.99 (brs, 1H); MS (APCI$^+$) $(M + H)^+$ at *m*/*z* 454, 456. Anal. ($C_{24}H_{24}ClN_3O_2S\cdot0.11H_2O$) C, H, N.

6-Chlorobenzimidazol-2-on-5-yl 2-Chloro-4-(*E*-((4-acetylpiperazin-1-yl)carbonyl)ethenyl)phenyl Sulfide (12). The potassium thiolate **7** (150 mg, 0.37 mmol) in 3.0 mL of DMF was heated with K_2CO_3 (76 mg, 0.55 mmol) and 4,5-dichloro-2-nitroaniline (76 mg, 0.37 mmol) at 70 °C for 3 h. Reaction was then quenched with water after cooling to room temperature. The yellow precipitates were collected through filtration, washed with water, and dried in a vacuum oven to give the nitro compound **11** (170 mg, 0.34 mmol, 93%).

To a stirred solution of nitrobenzene (170 mg, 0.34 mmol) in 2 mL of EtOH was added anhydrous $SnCl_2$ (325 mg, 1.72 mmol). The mixture was then refluxed for 2 h. The reaction was allowed to cool to ambient temperature, quenched with saturated $NaHCO_3$, and extracted with EtOAc (2 × 20 mL). The combined organic layer was washed with brine, dried over Na_2SO_4, and concentrated in vacuo. The residue was then purified on a Gilson preparative HPLC to give the dianilino compound as a light yellow solid (70 mg, 44%).

A mixture of dianiline (35 mg, 0.075 mmol) and CDI (13 mg, 0.075 mmol) in THF was stirred at ambient temperature for 1 day. Solvent was then removed under reduced pressure, and the crude product was purified on a Gilson preparative HPLC to give compound **12** (12 mg, 32%) as a white solid. ^{1}H NMR (DMSO-d_6, 300 MHz) δ 2.04 (s, 3H), 3.40−3.80 (m, 8H), 6.63 (d, J = 8.4 Hz, 1H), 7.11 (d, J = 2.4 Hz, 1H), 7.12 (s, 1H), 7.23 (s, 1H), 7.32 (d, J = 15.6 Hz, 1H), 7.43 (d, J = 15.6 Hz, 1H), 7.50 (d, J = 8.4 Hz, 1H), 8.03 (brs, 1H); MS (APCI$^+$) $(M - CO + H)^+$ at *m*/*z* 465, 467. Anal. ($C_{22}H_{20}Cl_2N_4O_3S\cdot0.16H_2O$) C, H, N.

Indol-6-yl 2-Chloro-4-(*E*-((4-acetylpiperazin-1-yl)carbonyl)ethenyl)phenyl Sulfide (17): white solid; ^{1}H NMR (DMSO-d_6, 300 MHz) δ 2.03 (s, 3H), 3.40−3.77 (m, 8H), 6.52−6.55 (m, 1H), 6.60 (d, J = 8.4 Hz, 1H), 7.13 (dd, J = 1.8, 8.4 Hz, 1H), 7.27 (d, J = 15.6 Hz, 1H), 7.40 (d, J = 15.6 Hz, 1H), 7.43 (dd, J = 1.8, 8.4 Hz, 1H), 7.51 (t, J = 3.0 Hz, 1H), 7.64 (m, 1H), 7.70 (d, J = 8.4 Hz, 1H), 7.99 (d, J = 1.8 Hz, 1H); MS

(APCI$^+$) $(M + H)^+$ at *m/z* 440, 442. Anal. ($C_{23}H_{22}ClN_3O_2S$·0.04TFA) C, H, N.

1-Methylindol-7-yl 2-Chloro-4-(*E*-((4-acetylpiperazin-1-yl)carbonyl)ethenyl)phenyl Sulfide (18): light brown solid; ^{1}H NMR ($CDCl_3$, 300 MHz) δ 2.14 (s, 3H), 3.47−3.56 (m, 2H), 3.56−3.83 (m, 6H), 3.96 (s, 3H), 6.42 (d, J = 8.4 Hz, 1H), 6.55 (d, J = 3.6 Hz, 1H), 6.76 (d, J = 15.6 Hz, 1H), 6.99 (d, J = 3.6 Hz, 1H), 7.09 (dd, J = 2.1, 8.4 Hz, 1H), 7.15 (t, J = 7.65 Hz, 1H), 7.42 (dd, J = 0.9, 7.5 Hz, 1H), 7.53 (d, J = 1.8 Hz, 1H), 7.55 (dd, J = 15.6 Hz, 1H), 7.77 (dd, J = 0.9, 7.5 Hz, 1H); MS (APCI$^+$) $(M + H)^+$ at *m/z* 454, 456. Anal. ($C_{24}H_{24}ClN_3O_2S$) C, H, N.

1-Ethylindol-7-yl 2-Chloro-4-(*E*-((4-acetylpiperazin-1-yl)carbonyl)ethenyl)phenyl Sulfide (19). Method B for Sulfide Formation. A stirred solution of thiolate **7** (65 mg, 0.18 mmol) in 1 mL of anhydrous DMSO was charged with 7-bromo-1-ethylindole (44 mg, 0.20 mmol), Pd $(PPh_3)_4$ (10.4 mg, 0.090 mmol), and *t*-BuONa (18 mg, 0.18 mmol). The mixture was heated in a sealed tube at 110 °C for 2 h. The reaction mixture was then cooled to room temperature and quenched with 3 mL of water. The crude product was extracted out with EtOAc (2 × 10 mL). The combined organic layer was then washed with water and brine, dried over Na_2SO_4, filtered, and concentrated. The desired product was isolated from a Gilson preparative HPLC as an off-white solid (19 mg, 0.041 mmol, 22%). ^{1}H NMR ($CDCl_3$, 300 MHz) δ 1.30 (t, J = 7.05 Hz, 3H), 2.14 (s, 3H), 3.52 (brs, 2H), 3.58−3.84 (m, 6H), 4.42 (q, J = 7.05 Hz, 2H), 6.42 (d, J = 8.4 Hz, 1H), 6.59 (d, J = 3.0 Hz, 1H), 6.76 (d, J = 15.6 Hz, 1H), 7.08 (d, J = 8.4 Hz, 1H), 7.10 (d, J = 3.0 Hz, 1H), 7.16 (t, J = 7.65 Hz, 1H), 7.42 (dd, J = 0.9, 7.5 Hz, 1H),7.53 (d, J = 1.8 Hz, 1H), 7.54 (d, J = 15.6 Hz, 1H), 7.78 (dd, J = 0.9, 7.5 Hz, 1H); MS (APCI$^+$) $(M + H)^+$ at *m/z* 468, 470. Anal. ($C_{25}H_{26}ClN_3O_2S$) C, H, N.

5-Methylenebenzodioxolyl 2-Chloro-4-(*E*-((4-acetylpiperazin-1-yl)carbonyl)ethenyl)phenyl Sulfide (20): white solid; ^{1}H NMR ($CDCl_3$, 300 MHz) δ 2.14 (s, 3H), 3.48−3.60 (m, 2H), 3.60−3.84 (m, 6H), 6.05 (s, 2H), 6.75 (d, J = 8.4 Hz, 1H), 6.80 (d, J = 15.3 Hz, 1H), 6.88 (d, J = 8.4 Hz, 1H), 6.98 (d, J = 2.1 Hz, 1H), 7.08 (dd, J = 2.1, 8.4 Hz, 1H), 7.19 (d, J = 1.8, 8.4 Hz, 1H), 7.52 (d, J = 2.1 Hz, 1H), 7.58 (d, J = 15.6 Hz, 1H); MS (APCI$^+$) $(M + NH_4)^+$ at *m/z* 445, 447. Anal. ($C_{22}H_{21}ClN_2O_4S$·0.12H_2O) C, H, N.

Benzodioxan-6-yl 2-Chloro-4-(*E*-((4-acetylpiperazin-1-yl)carbonyl)ethenyl)phenyl Sulfide (21): amorphous white solid; ^{1}H NMR ($CDCl_3$, 300 MHz) δ 2.14 (s, 3H), 3.44−3.57 (m, 2H), 3.57−3.86 (m, 6H), 4.25−4.35 (m, 4H), 6.75 (d, J = 8.4 Hz, 1H), 6.78 (d, J = 15.6 Hz, 1H), 6.93 (d, J = 8.4 Hz, 1H), 7.03 (dd, J = 2.1, 8.4 Hz, 1H), 7.08 (d, J = 2.1 Hz, 1H), 7.18 (dd, J = 2.1, 8.4 Hz, 1H), 7.51 (d, J = 2.1 Hz, 1H), 7.57 (d, J = 15.6 Hz, 1H); MS (APCI$^+$) $(M + H)^+$ at *m/z* 459, 461. Anal. ($C_{23}H_{23}ClN_2O_4S$·0.05H_2O) C, H, N.

1-Ethyl,3-(dimethylaminomethyl)indol-7-yl 2-Chloro-4-(*E*-((4-acetylpiperazin-1-yl)carbonyl)ethenyl)phenyl Sulfide (22): light-brown solid; ^{1}H NMR ($CDCl_3$, 300 MHz) δ 1.30 (t, J = 7.05 Hz, 3H), 2.14 (s, 3H), 2.41 (s, 6H), 2.93−3.05 (m, 2H), 3.47−3.55 (m, 2H), 3.55−3.87 (m, 6H), 6.42 (d, J = 8.4 Hz, 1H), 6.85 (d, J = 15.6 Hz, 1H), 7.09 (dd, J = 2.1, 8.4 Hz, 1H), 7.17 (d, J = 8.4 Hz, 1H), 7.23 (d, J = 8.4 Hz, 1H), 7.43 (dd, J = 0.9, 7.8 Hz, 1H), 7.52 (d, J = 2.1 Hz, 1H), 7.54 (d, J = 15.6 Hz, 1H), 7.81 (dd, J = 0.9, 7.8 Hz, 1H); MS (ESI$^+$) $(M + H)^+$ at *m/z* 525, 527. Anal. ($C_{28}H_{33}ClN_4O_2S$·1.09TFA) C, H, N.

1-(Carboxymethyl)indol-5-yl 2-Chloro-4-(*E*-((4-acetylpiperazin-1-yl)carbonyl)ethenyl)phenyl Sulfide (23). To a stirred solution of compound **8** (35 mg, 0.080 mmol) in 1 mL of anhydrous DMSO was added crushed KOH (18 mg, 0.32 mmol). After 45 min, *tert*-butyl bromoacetate (23.5 mL, 0.16 mmol) was added. The resulting mixture was stirred at ambient temperature for 10 h. Water was then added, and the reaction mixture was acidified with 3 N HCl to pH = 3. Acid **8** (25 mg, 63%) was isolated through filtration and drying in a vacuum oven as a white solid. ^{1}H NMR (DMSO-d_6, 300 MHz) δ 2.04 (s, 3H), 3.38−3.80 (m, 8H), 4.59 (s, 2H), 6.45 (d, J = 3.0 Hz, 1H), 6.52 (d, J = 8.7 Hz, 1H), 7.21 (dd, J = 2.1, 8.7 Hz, 1H), 7.25 (d, J = 15.6 Hz, 1H), 7.38 (d, J = 15.6 Hz, 1H), 7.40 (d, J = 3.0 Hz, 1H), 7.47 (d, J = 8.4 Hz, 1H), 7.80 (d, J = 2.1 Hz, 1H), 7.97 (s, 1H); MS (ESI$^+$) $(M - H)^+$ at *m/z* 496, 498. Anal. ($C_{25}H_{24}ClN_3O_4S$·0.18H_2O) C, H, N.

1-(2-Methoxyethyl)indol-5-yl 2-Chloro-4-(*E*-((4-acetylpiperazin-1-yl)carbonyl)ethenyl)phenyl Sulfide (24): white solid; ^{1}H NMR ($CDCl_3$, 300 MHz) δ 2.14 (s, 2H), 3.35 (s, 3H), 3.46−3.56 (m, 2H), 3.56−3.80 (m, 6H), 3.75 (t, J = 5.6 Hz, 2H), 4.33 (t, J = 5.6 Hz, 2H), 6.54 (d, J = 3.3 Hz, 1H), 6.61 (d, J = 8.7 Hz, 1H), 6.75 (d, J = 15.3 Hz, 1H), 7.09 (dd, J = 2.1, 11.7 Hz, 1H), 7.26 (overlapping d, 1H), 7.36 (dd, J = 2.1, 8.7 Hz, 1H), 7.44 (d, J = 8.7 Hz, 1H), 7.51 (d, J = 2.1 Hz, 1H), 7.56 (d, J = 15.3 Hz, 1H), 7.88 (d, J = 1.5 Hz, 1H); MS (ESI$^+$) $(M + H)^+$ at *m/z* 498, 500. Anal. ($C_{26}H_{28}ClN_3O_3S$·0.12 H_2O) C, H, N.

5-Ethoxybenzodioxan-6-yl 2-Chloro-4-(*E*-((4-acetylpiperazin-1-yl)carbonyl)ethenyl)phenyl Sulfide (25): white solid; ^{1}H NMR ($CDCl_3$, 300 MHz) δ 1.28 (t, J = 7.2 Hz, 3H), 2.14 (s, 3H), 3.54 (brs, 2H), 3.60−3.88 (m, 6H), 4.06 (q, J = 7.2 Hz, 2H), 4.33 (s, 4H), 6.70 (d, J = 8.4 Hz, 1H), 6.73 (d, J = 8.4 Hz, 1H), 6.78 (d, J = 15.6 Hz, 1H0, 6.98 (d, J = 8.4 Hz, 1H), 7.17 (dd, J = 1.8, 8.4 Hz, 1H), 7.50 (d, J = 1.8 Hz, 1H), 7.57 (d, J = 15.6 Hz, 1H); MS (APCI$^+$) $(M+H)^+$ at *m/z* 503, 505. Anal. ($C_{25}H_{27}ClN_2O_5S$·0.11H_2O) C, H, N.

2-(Hydroxymethyl)-benzodioxan-6-yl 2-Chloro-4-(*E*-((4-acetylpiperazin-1-yl)carbonyl)ethenyl)phenyl Sulfide (26): light yellow oil; ^{1}H NMR ($CDCl_3$, 300 MHz, mixture of 1:1 regioisomers) δ 2.15 (s, 3H), 3.46−3.83 (m, 8H), 3.83−4.01 (m, 2H), 4.10−4.42 (m, 4H), 6.75 (d, J = 8.4 Hz, 1H), 6.79 (d, J = 15.9 Hz, 1H), [6.95 (d), 6.98 (d), J = 4.8 Hz, 1H in total], [7.04 (t), 7.07 (t), J = 1.5 Hz, 1H in total], [7.10 (d), 7.11 (d), J = 2.4 Hz, 1H in total], 7.19 (d, J = 8.4 Hz, 1H), 7.53 (s, 1H), 7.58 (d, J = 15.6 Hz, 1H); MS (APCI$^+$) $(M + H)^+$ at *m/z* 489. Anal. ($C_{24}H_{25}ClN_2O_5S$·0.23H_2O) C, H, N.

2-Carboxy-benzodioxan-6-yl 2-Chloro-4-(*E*-((4-acetylpiperazin-1-yl)carbonyl)ethenyl)phenyl Sulfide (27): light brown solid; ^{1}H NMR (DMSO-d_6, 300 MHz, 1:1 mixture of regioisomers) δ 2.04 (s, 3H), 3.47 (brs, 6H), 3.55−3.77 (m, 2H), [5.01 (d), 5.03 (d), J = 5.1 Hz, 2H in total], [5.39 (brs), 5.43 (brs), 1H in total], [6.61 (d), 6.69 (d), J = 8.4 Hz, 1H in total], 6.73−6.95 (m, 2H), 6.95−7.23 (m, 2H), 7.24−7.60 (m, 2H), 7.92−8.01 (m, 1H); MS (ESI$^+$) $(M + Na)^+$ at *m/z* 503, 505. Anal. ($C_{24}H_{23}ClN_2O_6S$·0.15H_2O) C, H, N.

2-(Dimethylaminocarbonyl)-benzodioxan-6-yl 2-Chloro-4-(*E*-((4-acetylpiperazin-1-yl)carbonyl)ethenyl)phenyl Sulfide (28): white solid; ^{1}H NMR ($CDCl_3$, 300 MHz, 1:1 mixture of regioisomers) δ 1.93 (s, 3H), 2.15 (s, 6H), 3.53 (brs, 2H), 3.59−3.90 (brm, 8H), 4.86−5.01 (m, 1H), 6.74−6.81 (m, 1H), 6.80 (d, J = 15.3 Hz, 1H), 6.93 (d, J = 8.7 Hz, 1H), 7.02 (d, J = 1.8 Hz, 1H), 7.13 (dd, J = 1.8, 8.4 Hz, 1H), 7.16−7.25 (m, 1H), 7.54 (s, 1H), 7.58 (d, J = 15.6 Hz, 1H); MS (ESI$^+$) $(M + Na)^+$ at *m/z* 552, 554. Anal. ($C_{26}H_{28}ClN_3O_5S$·0.35H_2O) C, H, N.

5-Chloro-8-ethoxyquinolin-7-yl 2-Chloro-4-(*E*-((4-acetylpiperazin-1-yl)carbonyl)ethenyl)phenyl Sulfide (29): white solid; ^{1}H NMR (DMSO-d_6, 300 MHz) δ 1.37 (t, J = 7.2 Hz, 3H), 2.04 (s, 3H), 3.41−3.82 (m, 8H), 4.46 (q, J = 7.2 Hz, 2H), 7.29 (s, 1H), 7.37 (d, J = 8.4 Hz, 1H), 7.42 (d, J = 15.6 Hz, 1H), 7.51 (d, J = 15.6 Hz, 1H), 7.68 (dd, J = 1.8, 8.4 Hz, 1H), 7.74 (dd, J = 3.9, 8.4 Hz, 1H), 8.15 (s, 1H), 8.55 (dd, J = 1.8, 8.4 Hz, 1H), 9.05 (dd, J = 1.8, 3.9 Hz, 1H); MS (APCI$^+$) $(M + H)^+$ at *m/z* 530, 532, 534. Anal. ($C_{26}H_{25}Cl_2N_3O_3S$·0.28TFA) C, H, N.

Aqueous Solubility Determination. The compound was suspended in a phosphate buffer (pH 7.4, ion strength adjusted to 0.15 M with sodium chloride). This suspension was equilibrated by rotating at 25 rpm for approximately 2 d at 25 °C. The excess solid was removed by filtration. The resulting saturated solution was diluted and analyzed for drug concentration by UV spectrophotometry.

For ICAM-1/LFA-1 biochemical interaction assay, ICAM-1/JY-8 cell adhesion assay, and pharmacokinetic analysis protocols, see the preceding paper in the series.[13]

Acknowledgment. The authors thank the Abbott Analytical Department for assistance in acquiring ^{1}H

NMR and mass spectra, Bach-Nga Nguyen and Kennan Marsh of the Drug Analysis Department for obtaining rat pharmacokinetic data, and Yi Gao of the Preformulation Department for determining the aqueous solubility data.

References

(1) Springer, T. A. Traffic Signals for Lymphocyte Recirculation and Leukocyte Emigration: the Multistep Paradigm. *Cell* **1994**, *76*, 301−314.
(2) Hynes, R. O. Integrins: Versatility, Modulation, and Signaling in Cell Adhesion. *Cell* **1992**, *69*, 11−25.
(3) Gahmberg, C. G. Leukocyte Adhesion: CD11/CD18 Integrins and Intercellular Adhesion Molecules. *Curr. Opin. Cell. Biol.* **1997**, *9*, 643−650.
(4) Carlos, T. M.; Harlan, J. M. Leukocyte-Endothelial Adhesion Molecules. *Blood* **1994**, *84*, 2068−2101.
(5) Ley, K. Molecular Mechanisms of Leukocyte Recruitment in the Inflammatory Process. *Cardiovasc. Res.* **1996**, *30*, 733−742.
(6) Sligh, J. E.; Ballantyne, C. M.; Rich, S. S.; Hawkins, H. K.; Smith, C. W.; Bradley, A.; Beaudet, A. L. Inflammatory and Immune Responses Are Impaired in Mice Deficient in Intercellular Adhesion Molecule 1. *Proc. Natl. Acad. Sci. U.S.A.* **1993**, *90*, 8529−8533.
(7) (a) Hourmant, M.; Le Mauff, B.; Le Meur, Y.; Dantal, J.; Cantarovich, D.; Giral, M.; Caudrelier, P.; Albericci, G.; Soulilou, J. P. Administration of an Anti-CD11a Monoclonal Antibody in Recipients of Kidney Transplantation: a Pilot Study. *Transplantation* **1994**, *58*, 377−380. (b) Nakakura, E. K.; Shorthouse, R. A.; Zheng, B.; McCabe, S. M.; Jardieu, P. M.; Morris, R. E. Long-term Survival of Solid Organ Allografts by Brief Anti-Lymphocyte Function-associated Antigen-1 Monoclonal Antibody Monotherapy. *Transplantation* **1996**, *62*, 547−552.
(8) (a) Lee, J.-O.; Rieu, P.; Arnout, M. A.; Liddington, R. C. Crystal Structure of the A Domain from the α-Subunit of the Integrin CR3 (CD11b/CD18). *Cell* **1995**, *80*, 631−638. (b) Lee, J.-O.; Bunkston, L. A.; Arnout, M. A.; Liddington, R. C. Two Conformations of the Integrin A-Domain (I-domain): a Pathway for Activation? *Structure* **1995**, *3*, 1333−1340.
(9) Qu, A.; Leahy, D. J. Crystal Structure of the I-domain from CD11a/CD18. *Proc. Natl. Acad. Sci. U.S.A.* **1995**, *92*, 10277−10281.
(10) Qu, A.; Leahy, D. J. The Role of the Divalent Cation in the Structure of the I-Domain from the CD11a/CD18 Integrin. *Structure* **1996**, *4*, 931−942.
(11) Emsley, J.; Knight, C. G.; Farndale, R. W.; Barnes, M. J.; Liddington, R. C. Structural Basis of Collagen Recognition by Integrin $\alpha_2\beta_1$. *Cell* **2000**, *101*, 47−56.
(12) Huth, J. R.; Olejniczak, E. T.; Mendoza, R.; Liang, H.; Harris, E. A.; Lupher, Jr., M. L.; Wilson, A. E.; Fesik, S. W.; Staunton, D. E. NMR and Mutagenesis Evidence for an I Domain Allosteric Site that Regulates Lymphocyte Function-associated Antigen-1 Ligand Binding. *Proc. Natl. Acad. Sci. U.S.A.* **2000**, *97*, 5231−5236.
(13) Liu, G.; Link, J. T.; Pei, Z.; Reilly, E. B.; Leitza, S.; Nguyen, B.; Marsh, K. C.; Okasinski, G. F.; von Geldern, T. W.; Ormes, M.; Fowler, K.; Gallatin, M.; Discovery of Novel *p*-Arylthio Cinnamides as Antagonists of Leukocyte Function-associated Antigen-1/Intracellular Adhesion Molecule-1 Interaction. 1. Identification of an Additional Binding Pocket Based on an Anilino Diaryl Sulfide Lead. *J. Med. Chem.* **2000**, *43*, 4025−4040.
(14) Migita, T.; Shimizu, T.; Asami, Y.; Shiobara, J.; Kato, Y.; Kosugi, M. The Palladium Catalyzed Nucleophilic Substitution of Aryl Halides by Thiolate Anions. *Bull. Chem. Soc. Jpn.* **1980**, *53*, 1385−1389.
(15) Šindelár, K.; Kmonícek, V.; Hrubantová, M.; Polívka, Z. Substituted *N*,*N*-Dimethyl-(3-phenylthio)- and -4-(Phenylthio)benzylamines. *Collect. Czech. Chem. Commun.* **1992**, *57*, 194−203.
(16) Kay, L. E.; Keifer, P.; Saarinen, T. Pure Absorption Gradient Enhanced Heteronuclear Single Quantum Correlation Spectroscopy with Improved Sensitivity. *J. Am. Chem. Soc.* **1992**, *114*, 10663−10665.
(17) Kallen, J.; Welzenbach, K.; Ramage, P.; Geyl, D.; Kriwacki, R.; Legge, G., Cottens, S.; Weitz-Schmidt, G.; Hommel, U. Structural Basis for LFA-1 Inhibition upon Lovastatin Binding to the CD11a I-domain. *J. Mol. Biol.* **1999** *292*, 1−9.
(18) Hajduk, P. J.; Gomtsyan, A.; Didomenico, S.; Cowart, M.; Bayburt, E. K.; Solomon, L.; Severin, J.; Smith, R.; Walter, K.; Holzman, T. F.; Stewart, A.; McGaraughty, S.; Jarvis, M. F.; Kowaluk, E. A.; Fesik, S. W. Design of Adenosine Kinase Inhibitors from the NMR-based Screening of Fragments. *J. Med. Chem.* **2000**, 43, 4781−4786.
(19) Liu, G.; Wang, G.; Wang, S. Unpublished results.
(20) Anzali, S.; Mederski, W. W. K. R.; Osswald, M.; Dorsch, D. Endothelin Antagonists: Search for Surrogates of Methylendioxypenyl by Means of a Kohonen Neural Network. *Bioorg. Med. Chem. Lett.* **1998**, *8*, 11−16.
(21) Olejniczak, E. T.; Hajduk, P. J.; Marcotte, P. A.; Nettesheim, D. G.; Meadows, R. P.; Edalji, R.; Holzman, T. F.; Fesik, S. W. Stromelysin Inhibitors Designed from Weakly Bound Fragments: Effects of Linking and Cooperativity. *J. Am. Chem. Soc.* **1997**, *119*, 5828−5832.
(22) Hajduk, P. J.; Sheppard, G.; Nettesheim, D. G.; Olejniczak, E. T.; Shuker, S. B.; Meadows, R. P.; Steinman, D. H.; Carrera, G. M.; Marcotte, P. A.; Severin, J.; Walter, K.; Smith, H.; Gubbins, E.; Simmer, R.; Holzman, T. F.; Morgan, D. W.; Davidsen, S. K.; Fesik, S. W. Discovery of Potent Nonpeptide Inhibitors of Stromelysin Using SAR by NMR. *J. Am. Chem. Soc.* **1997**, *119*, 5818−5827.
(23) Gardner, K. H.; Kay, L. E. Production and Incorporation of ^{15}N, ^{13}C, ^{2}H (^{1}H-δ1 Methyl) Isoleucine into Proteins for Multidimensional NMR Studies. *J. Am. Chem. Soc.* **1997**, *119*, 7599−7600.
(24) Gemmecker, G.; Olejniczak, E. T.; Fesik, S. W. An Improved Method for Selectively Observing Protons Attached to ^{12}C in the Presence of ^{13}C-^{1}H Spin Pairs. *J. Magn. Reson.* **1992**, *96*, 199−204.
(25) Gronenborn, A. M.; Clore, G. M. Structures of Protein Complexes by Multidimensional Heteronuclear Magnetic Resonance Spectroscopy. *Crit. Rev. Biochem. Mol. Biol.* **1995**, *30*, 351−385.
(26) Brunger, A. T. *X-PLOR Version 3.1.*; Yale University Press: New Haven and London, 1992.

JM000503F